European Journal of Radiology 121 (2019) 108710

Contents lists available at ScienceDirect

European Journal of Radiology

journal homepage: www.elsevier.com/locate/ejrad

Clinical evaluation of a fully-automated parenchymal analysis software for breast cancer risk assessment: A pilot study in a Finnish sample

Said Pertuz[a,b,*], Antti Sassi[c], Kirsi Holli-Helenius[c], Joni Kämäräinen[b], Irina Rinta-Kiikka[c], Anna-Leena Lääperi[c], Otso Arponen[d]

[a] Connectivity and Signal Processing group, Universidad Industrial de Santander, 680002 Bucaramanga, Colombia
[b] Computing Sciences, Tampere University, 33710 Tampere, Finland
[c] Department of Radiology, Tampere University Hospital, 33521 Tampere, Finland
[d] Department of Oncology, Tampere University Hospital, 33521 Tampere, Finland

ARTICLE INFO

Keywords:
Breast cancer
Risk assessment
Parenchymal analysis
Texture analysis
Imaging biomarker

ABSTRACT

Purpose: To assess the association between breast cancer risk and mammographic parenchymal measures obtained using a fully-automated, publicly available software, OpenBreast.

Methods: This retrospective case-control study involved screening mammograms of asymptomatic women diagnosed with breast cancer between 2016 and 2017. The 114 cases were matched with corresponding healthy controls by birth and screening years and the mammographic system used. Parenchymal analysis was performed using OpenBreast, a software implementing a computerized parenchymal analysis algorithm. Breast percent density was measured with an interactive thresholding method. The parenchymal measures were Box-Cox transformed and adjusted for age and percent density. Changes in the odds ratio per standard deviation (OPERA) with 95% confidence intervals (CIs) and the area under the ROC curve (AUC) for parenchymal measures and percent densities were used to evaluate the discrimination between cases and controls. Differences in AUCs were assessed using DeLong's test.

Results: The adjusted OPERA value of parenchymal measures was 2.49 (95% CI: 1.79–3.47). Parenchymal measures using OpenBreast were more accurate (AUC = 0.779) than percent density (AUC = 0.609) in discriminating between cases and controls ($p < 0.001$).

Conclusions: Parenchymal measures obtained with the evaluated software were positively associated with breast cancer risk and were more accurate than percent density in the prediction of risk.

1. Introduction

From a global perspective, breast cancer is the most common cancer in women and ranks second as a cause of cancer deaths in the developed regions [1]. Personalized screening recommendations to reduce mortality rates have been investigated to offer tailored screening regimens to women according to individual risk levels [2]. Effective risk assessment methods based on different techniques and imaging modalities are being developed [3]. In this respect, mammographic screening, due to its relatively low cost, ease of acquisition and widespread use, has considerable potential not only for the detection of suspicious lesions but also for the identification of women at high risk [4].

There is convincing experimental evidence for an association between parenchymal measures and the breast cancer risk [5]. Interestingly, recent studies have indicated that parenchymal measures are associated with breast cancer risk independently of breast density [6]; parenchymal methods are potentially better than breast density measurements in revealing the complexity of breast tissue [7]. The classical approach for parenchymal analysis can be summarized in three steps: identification of a region of interest (ROI) within the breast, extraction of different measures in the ROI by means of computerized texture descriptors, and the construction of a risk scoring model based on machine learning [8]. See [5] for a comprehensive review of algorithms developed and tested in breast cancer risk assessment.

The ROI placement (parenchymal / whole breast) and the selection of texture descriptors remain open problems. The uncertain

Abbreviations: AUC, area under the receiver operating characteristic curve; FFDM, full-fielddigital mammography; IQR, inter-quartilerange; OPERA, odds per adjusted standard deviation; PD, percent density

* Corresponding author at: Universidad Industrial de Santander, Calle 9, carrera 27, 680002 Bucaramanga, Colombia.
E-mail address: spertuz@uis.edu.co (S. Pertuz).

https://doi.org/10.1016/j.ejrad.2019.108710
Received 25 July 2019; Received in revised form 4 October 2019; Accepted 11 October 2019

reproducibility of parenchymal measures remains an important obstacle to be overcome before embarking on phase II and III studies. The aim of this case-control study was to evaluate the association between the breast cancer risk and parenchymal measures computed using OpenBreast, a new freely and publicly available software implementing a parenchymal analysis algorithm [8]. We hope that this will facilitate the development of a consensus regarding the utilization of parenchymal analysis algorithms for risk assessment and expanding their clinical applications. As an alternative to parenchymal analysis, some researchers have recently also examined the benefits of deep learning methods for breast cancer risk assessment based on mammograms [9,6,10]. Although these approaches have shown promising results, these models are not publicly available. Therefore, here our scope was limited to classical parenchymal analysis methods.

2. Materials and methods

This study was conducted within the screening program of Tampere University Hospital. The hospital has the screening responsibilities for the inhabitants of two municipalities in the Pirkanmaa Region, Finland. The Government Decree on Screenings mandates that municipalities should send a regular, biannual invitation to mammographic breast cancer screening to all women aged between 50–69 years living in Finland. All mammograms are read by two breast radiologists trained in screening mammography.

Screening patient flow in our institution is managed using the Optomed Software (Optomed Ltd, Finland). All patients diagnosed with screening-detected breast cancers were retrieved from the patient flow management software. We have assessed all 172 women with breast cancers detected in screening in the years 2016 and 2017. The inclusion criteria for the cases were: 1) no known history of previously detected breast malignancies or previous invasive operations in the field of view (e.g. lumpectomy, mastectomy, breast implant, coiling, pacemaker) as these were hypothesized to have an impact on breast parenchyma, and 2) no reported breast-cancer related symptoms as they would require further management irrespective of the mammographic result. Patients were also excluded if there was a biopsy-warranting lesion in the contralateral breast because the contralateral breast was used for image analysis. Patients who did not meet the inclusion criteria or had an exclusion criterion were excluded (N = 58). The patient selection flowchart is shown in Fig. 1. Table 1 summarizes histopathological diagnoses and tumor characteristics of the cases examined in this study.

We searched for consecutive healthy controls matched by screening and birth years and imaged with the same mammography system. Women with a known history of breast malignancies, previous invasive operations or the need for further biopsies were excluded. After the selection, the study sample consisted of mammograms of 114 patients (“cases”) with screening-detected asymptomatic cancers and 114 matched consecutive healthy women (“controls”).

In compliance with local and national regulations and laws, the use of register data including mammographic images and patient history was approved and the need for informed consent was waived by the local chair of the Tampere University Hospital district. This retrospective study did not change either the diagnostic decisions or the management of the patients. Patient history (women’s age, breast cancer characteristics (including histopathology and tumor size)) was retrieved from the electronic patient charts.

2.1. Mammographic systems and image retrieval

Bilateral two-view cranio-caudal (CC) and mediolateral oblique (MLO) full-field digital mammography (FFDM) images from each breast were acquired using either a MicroDose SI (Philips Healthcare, the Netherlands) or a Senographe Essential (General Electric Medical Systems, USA) mammography system. Approximately 350 women per week are screened at our institution. The choice of the system was based on the availability and the screening mammography was performed by a non-associated mammographer trained in mammographic screening. In clinical practice, images are customarily captured with different imaging parameters that include both acquisition-specific and system-specific parameters such as the compressed breast thickness, compression force, X-ray tube voltage peak, and target-filter combination. Therefore, one could expect parenchymal measures computed from images obtained using different imaging systems to exhibit some differences [11]. We controlled for the effect of the imaging parameters by matching cases and controls according to which mammographic system had been used in their assessment.

Images were saved to the Sectra Workstation IDS7 (version 18.1, Sectra, Sweden) PACS and the radiologists used Optomed Software (Optomed Ltd, Finland) to manage the image workflow. The mammograms were downloaded from the Sectra Workstation IDS7 PACS. We collected the CC view images of the unaffected contralateral breast of the patients diagnosed with cancer. The utilization of images of the contralateral, unaffected breast at the time of diagnosis as a surrogate of images from previous screening rounds is a common practice in the evaluation of computerized imaging biomarkers [12–15]. In particular, the use of images from the contralateral breast avoids problems due to missing retrospective imaging data and changes in imaging technologies [12–15]. Recent studies have demonstrated that there are no statistically significant differences between CC or MLO views when used for parenchymal analysis [16]. We chose the contralateral CC view mammogram for cases in this analyses in order to avoid noise or artifacts due to faulty chest wall detection in the MLO view [16]. The right breast CC view mammogram was used in the analyses of healthy controls. All images were *processed* digital mammograms stored in a 16-bit format. All images were standardized to a resolution of 0.1 mm/pixel by digitally resizing mammograms according to each system’s pitch because different mammographic systems have varying resolutions.

2.2. Parenchymal analysis

The parenchymal analysis was performed by one of its developers (S.P) using OpenBreast v1.0 (Universidad Industrial de Santander, Colombia); this is a publicly available software that incorporates the most recent advances in parenchymal analysis [8]. OpenBreast has not been clinically validated and was developed using imaging data different from this study. Briefly, parenchymal analysis is performed automatically in three steps following the classical approach for parenchymal analysis: ROI detection, feature extraction and risk estimation. First, the ROI detection aims to delineate the full breast region from the background of the mammogram and to automatically localize a ROI within the breast for subsequent analysis. In the literature, different ROIs have been considered for the parenchymal analysis including the whole breast [17], the largest circumscribed squared region within the breast [12], the retro-areolar region [14,18], and multiple individual regions [13]. OpenBreast is able to perform a feature extraction from all of the above-mentioned regions. It remains an open question which is the most suitable region of interest for the risk analysis. We used the whole breast for the analysis based on our preliminary experiments; the breast region was detected by thresholding the mammogram to remove the highest mode of the image historgram as described previously [19]. Feature extraction, i.e. computation of a series of quantitative measurements (features) within the breast ROI aims to characterize spatial parenchymal patterns [13]. In addition to computational features, imaging parameters related to the mammographic system (compressed breast thickness, compression force, X-ray tube voltage peak and target-filter combination) are included in the analysis. OpenBreast computes a total 37 different features for each mammogram. The final step, risk scoring, exploits classical machine learning in order to calculate each woman’s risk level based on the extracted features. OpenBreast generates a report with the estimated risk score R that lies within the range of 0–1, where 0 and 1 correspond

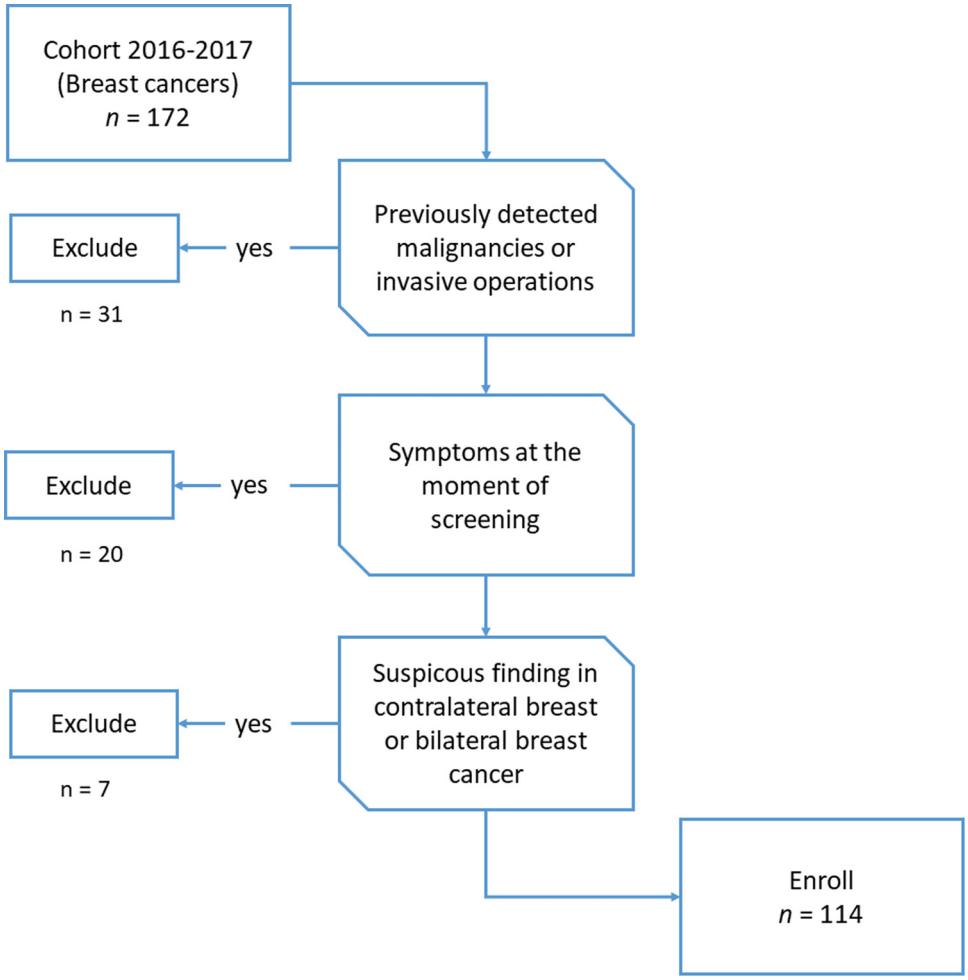

Fig. 1. Diagram describing the selection of cases examined in this study.

Table 1
Histopathological diagnoses and characteristics of the tumors.

Characteristics	N	%
Histopathology		
Non-invasive		
DCIS*	22	19
Invasive		
Ductal	74	65
Lobular	14	12
Mucinous	2	2
Mixed ducto-lobular	1	1
Tubular	1	1
T classification		
Tis*	22	19
T1	75	66
T2	16	14
T3	1	1
T4	0	0

* Including one DCIS lesion with microinvasion.

to the lowest and highest risk levels, respectively. The full dataset (N = 228) was split into independent training and test sets by using 5-fold cross validation stratified by the mammographic system. In each run, the images in the training sets were utilized for building a risk model and the images in the test set were used to evaluate the performance.

2.3. Density estimation

Breast percent density was computed using a Cumulus-like interactive thresholding technique [20–22]. This technique allows a human reader to segment dense parenchymal tissue from non-dense tissue by manually adjusting the intensity threshold in the mammogram (Fig. 2). Percent density (PD) is then calculated automatically by computing the relative amount of dense tissue over the whole breast area. To reduce the effect of inter-reader variance, the estimation of breast density was performed simultaneously by two readers with 1 to 2 years of experience in mammographic imaging (O. A and A. S) blinded to any information of the R score and whether the image belonged to a case or a control subject. All segmentations were subsequently reviewed and approved by a breast radiologist with over 20 years of experience in breast imaging (A. L). This process was repeated for every mammogram until the three parties (O.A, A. S and A. L) were satisfied with the segmentations.

2.4. Statistical analysis

Non-normally distributed continuous variables are presented as medians with interquartile ranges, and categorical variables are presented as absolute values and percentages. We used the Box-Cox power transformation to normalize both the R and PD distributions [23]. Subsequently, we standardized all the transformed measures by subtracting the means and normalizing them according to their standard deviations. We used the standardized transformed measures to evaluate the association with the breast cancer risk using the odds per adjusted

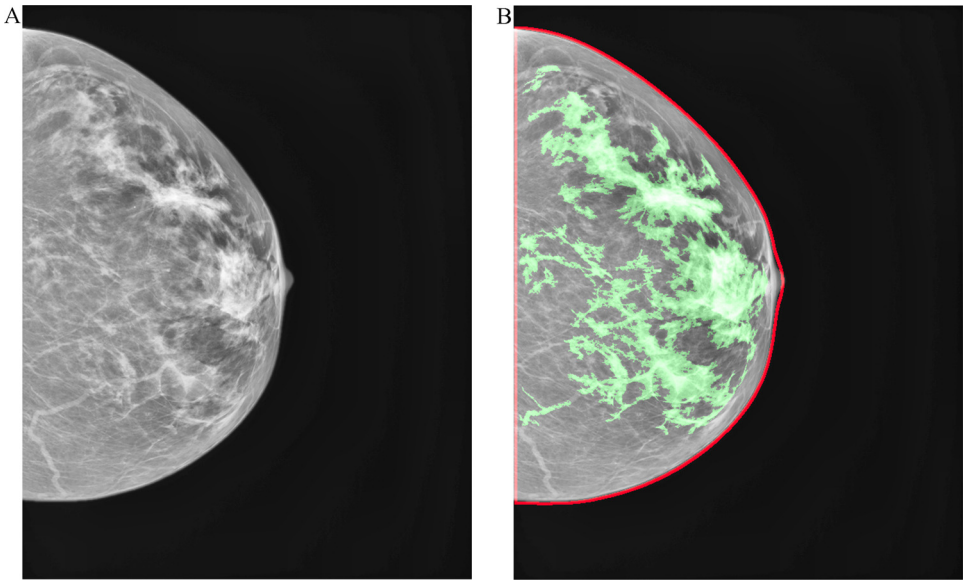

Fig. 2. Breast percent density estimation using an interactive thresholding method. The dense tissue is segmented by manually adjusting the intensity threshold in the mammogram. **(a)** Original mammography image. Right CC view of a 68-year-old woman diagnosed with breast cancer. **(b)** Segmented dense tissue using interactive thresholding (PD = 30%). The red line indicates the breast delineation and the green color marks the parenchymal segment.

standard deviation (OPERA) [24], with 95% confidence intervals (CI). An OPERA value measures how well a risk factor differentiates "high risk" (cases) from "low risk" (control) women. OPERA values have been previously utilized to compare the predictive power of different density estimation methods [25]. We used the area under the receiver operating characteristic curve (AUC) with a stratified 5-fold cross validation without replacement for the assessment of the accuracy of the risk prediction. The differences in AUCs were assessed using DeLong's test [26]. Both the risk score (R) and percent density (PD) were non-normally-distributed and therefore Mann-Whitney U test was used to evaluate statistical differences in these two measurements between the case and control groups. A p value less than 0.05 was considered to indicate statistical significance. The statistical analyses were performed using Matlab 2017b (Mathworks Inc., the USA).

3. Results

In the study sample, 48% (N = 110) of the mammograms were acquired using a Philips mammographic system and 52% (N = 118) with the GE mammographic system. The median age of the women was 60 years (range 50–68 years). Patient and control characteristics are summarized in Table 2.

3.1. Risk measures and breast cancer risk

Before the Box-Cox transformation, the median parenchymal scores and interquartile ranges (IQRs) of the case and control groups were R = 0.94 (IQR: 0.27-0.99) and R = 0.20 (IQR: 0.07-0.47), respectively. The medians and interquartile ranges for percent densities in the case and control groups were PD = 29% (IQR: 22–38%) and PD = 23% (18–32%), respectively. Both risk measures, i.e. the risk score and the breast percent density, showed statistically significant differences in their distributions between the case and control groups (the Mann-Whitney U test, $p < 0.001$ and $p = 0.004$, respectively). Risk scores and density measures were not correlated (Spearman's $\rho = 0.11$, $p = 0.0711$).

When used alone as imaging biomarkers, both parenchymal measures and percent density showed positive associations with the breast cancer risk with OPERA values of 2.51 (95% CI: 1.81–3.49, $p < 0.001$) and 1.39 (95% CI: 1.06–1.82, $p = 0.01$), respectively. After adjusting for density, parenchymal measures retained their statistical significance with an OPERA value of 2.49 (95% CI: 1.79–3.47, $p < 0.001$). Fig. 3 shows estimated risk scores for different mammograms with different densities.

Table 2
Characteristics of the subjects. Density and risk quartiles were established according to the distributions of these values among control subjects.

Characteristic	Cases (%) N = 114	Controls (%) N = 114
Mammographic system		
Philips*	55 (48)	55 (48)
GE**	60 (52)	60 (52)
Age at mammography (years)		
< 55	26 (23)	26 (23)
55-59	21 (18)	21 (18)
60-64	44 (38)	44 (38)
> 64	24 (21)	24 (21)
Breast percent density		
Q1: < 18%	17 (15)	29 (25)
Q2: 18-23%	19 (17)	28 (25)
Q3: 23-32%	32 (28)	29 (25)
Q4: > 32%	47 (41)	29 (25)
Breast thickness (mm)		
Q1: < 51.0	24 (21)	26 (23)
Q2: 51.0-58.5	29 (25)	31 (27)
Q3: 58.5-66.0	31 (27)	28 (25)
Q4: > 66.0	30 (26)	29 (25)
Risk scores		
Q1: < 0.07	11 (10)	28 (25)
Q2: 0.07-0.20	15 (13)	29 (25)
Q3: 0.20-0.47	10 (9)	28 (25)
Q4: > 0.47	78 (68)	29 (25)

Q1-Q4 = quartiles.1–4.
* MicroDose SI (Philips Healthcare, the Netherlands).
** Senographe Essential (GE Medical Systems, the USA).

3.2. Differentiation between cases and controls

The AUCs for the assessment of the accuracy of parenchymal measures of the percent density in the differentiation of healthy controls and women diagnosed with breast cancer were 0.779 and 0.609 (Fig. 4), respectively; these differences were statistically significant ($p = 0.001$). Incorporation of age and PD to parenchymal measures achieved an increase in accuracy in comparison to unadjusted parenchymal measures (AUC = 0.786), although the improvement was not statistically significant ($p = 0.462$).

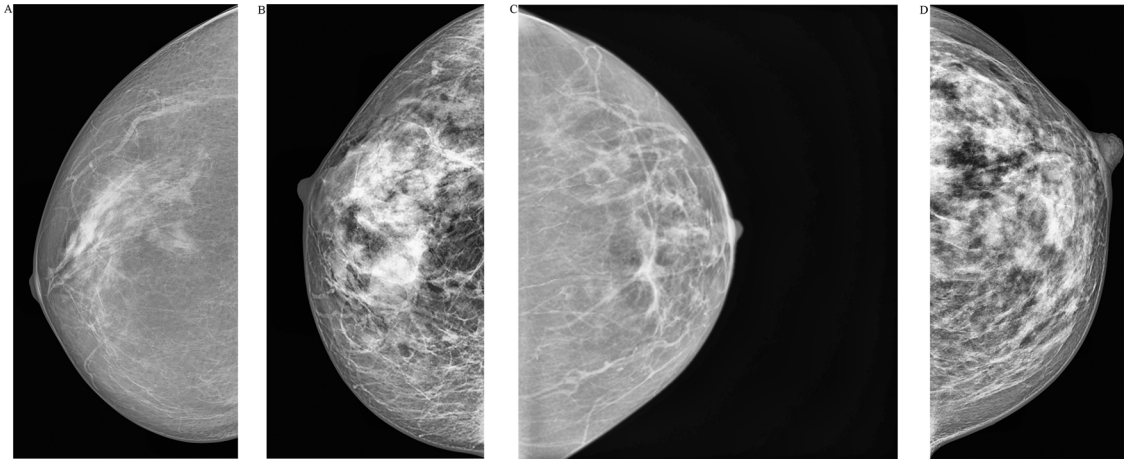

Fig. 3. Mammograms with different percent densities and risk scores. **(a)** A woman from the control group with a low breast density and a low risk score (Age 55 years, PD = 15%, R = 0.11). **(b)** A woman from the control group with a high density and a low risk score (Age 55 years, PD = 52%, R = 0.16). **(c)** A woman from the case group with a low density and a high risk score (Age 58 years, PD = 12%, R = 0.90). **(d)** A woman from the case group with a high density and a high risk score (Age 55 years, PD = 64%, R = 0.96).

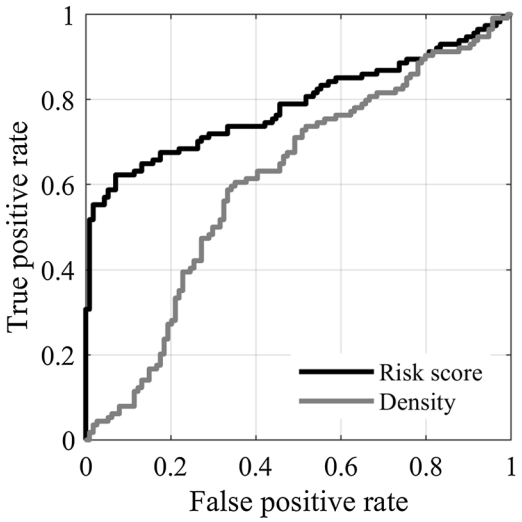

Fig. 4. ROC curves of breast density and parenchymal risk scores in the prediction of breast cancer risk.

4. Discussion

In this retrospective case-control study, the computerized parenchymal measures from FFDM images obtained using OpenBreast were positively associated with the breast cancer risk after taking density and age into account. A recent meta-analysis of more than 40 studies showed that parenchymal measures are positively associated with the breast cancer risk [5]. Our results are in line with the findings in several publications [12,6,18,17] and indicate that parenchymal patterns are more predictive of the breast cancer risk than the corresponding assessment of percent density.

The majority of breast cancers occur in women who have average or moderately elevated risk of breast cancer (≤ 20% lifetime risk of developing breast cancer). Indeed, according to the literature, only 5–10 % of women have genetic predisposition to breast cancer [27]. A topic attracting growing interest is the development of means to tailor screening regimens to women according to their individual risk levels [2]. Increased breast density has been associates with higher breast cancer risk [28]. Nevertheless, the major organizations (e.g. The American College of Radiology, The European Society of Breast Imaging, The National Comprehensive Cancer Network, The European Society for Medical Oncology) do not recommend interval-intensified screening solely based on breast density. There is a growing body of evidence that parenchymal measures outperform the density measures in risk prediction and represent candidate biomarkers that could enable risk-driven screening [12,6,18,17]. In this respect, further research on automatic tools, such as OpenBreast, is warranted.

In the literature, there are a few publicly available and widely utilized tools for the estimation of breast density, such as *VolparaDensity* (Volpara Solutions, ND) [29], LIBRA [30] or QUANTRA [31]. However, we are aware of only two other software tools which perform a risk assessment based on parenchymal analysis: BreastIQ and CaPTk [32,33]. BreastIQ is a software developed by Biomediq A/S; although we did not find clinical studies specifically for BreastIQ, the same company evaluated a prototype software in a prospective setting with promising results [6]. In that work, mammographic texture patterns were positively associated with breast cancer with hazard risk ratios of up to 3.16 when comparing women in the fourth quartile vs. those in the first quartile. CaPTk is a software capable of performing an analysis of radiographic brain, lung and breast images [34]. CaPTk is the result of a continuous, ongoing effort in the development of quantitative mammographic image analysis tool for the assessment of breast cancer risk [35]. We did not find any clinical studies which have used CaPTk specifically in the assessment of breast cancer risk, but the original developers of the parenchymal analysis pipeline reported AUCs of up to 0.85 in a case-control study with 106 cases and 318 age-matched controls [13]. Our results suggest that parenchymal measures obtained with OpenBreast have the potential to be utilized as an imaging biomarker to estimate the risk of breast cancer independently of breast density. We hope that our results will be validated by independent researchers and furthermore, while it would be interesting to compare OpenBreast with other tools, one notable advantage of OpenBreast is that this software is a non-commercial and publicly open tool.

There are several limitations to this study. Factors that may associate with parenchymal measures are poorly recognized, and they are considered to reflect independent biological risk factors associated with cancer development [17]. We took age and breast density into consideration as potential confounding factors in the parenchymal measures. Associations between parenchymal measures, clinical features and genetic factors should be studied in more detail as this might clarify our understanding of the potential benefits – and the limitations – of parenchymal measures. Secondly, it is well established that there is extensive inter- and intra-reader variability in the visual assessment of breast density [36,37]. Three experienced readers evaluated the PD measurements in order to reduce the effect of inter-reader variability. Inaccuracies in the estimation of density could result in an

underestimation of the discriminatory power of breast density. The sample size in this case-control study was relatively small. However, we believe that the sample is relatively representative as the majority of eligible women were older than 60 years. Furthermore, the proportion of non-invasive breast cancers to invasive breast cancers is in agreement with published estimates [38]. The proportions of the major histopathological subtypes (ductal and lobular carcinomas and ductal carcinoma in situ) were appropriately present in the cohort [39]. Finally, we conducted the study in a case-cohort setting with concurrent contralateral mammograms for risk prediction. Although such an approach has been used in studies estimating density-based and parenchymal-based risk, ithas the potential of being unrepresentative in screening populations. The practice of using concurrent images may cause the inclusion of mammograms with undetected lesions. Larger studies in prospective randomized controlled settings to examine whether parenchymal measures can predict accurately the future breast cancer risk will be needed before the modified screening regime trials can be approved.

To conclude, this study showed that computerized parenchymal measures from FFDM images were positively associated with the breast cancer risk after taking density and age into account. Parenchymal measures outperformed percent density in the differentiation between high-risk and low-risk women. OpenBreast is a publicly available software that potentially may be used to predict the breast cancer risk.

Declaration of Competing Interest

The authors declare no conflicting interests

Acknowledgements

S. Pertuz was partially funded by project VIE1563 “Análisis espacial de densidad en mamografía digital para la evaluación de riesgo de cáncer de seno” of Universidad Industrial de Santander.

Appendix A. Supplementary data

Supplementary material related to this article can be found, in the online version, at doi:https://doi.org/10.1016/j.ejrad.2019.108710.

References

[1] J. Ferlay, I. Soerjomataram, R. Dikshit, S. Eser, C. Mathers, M. Rebelo, D.M. Parkin, D. Formany, F. Bray, Cancer incidence and mortality worldwide: sources, methods and major patterns in GLOBOCAN 2012, Int. J. Cancer 136 (2014) E359–E386.
[2] T. Onega, E.F. Beaber, B.L. Sprague, W.E. Barlow, J.S. Haas, A.N. Tosteson, M.D. Schnall, K. Armstrong, M.M. Schapira, B. Geller, D.L. Weaver, E.F. Conant, Breast screening in the era of personalized regimens, Cancer 120 (19) (2014) 2955–2964.
[3] J.R. Harris, M.E. Lippman, M. Morrow y, C.K. Osborne, Diseases of the Breast, 5 ed., Wolters Kluwer, Philadelphia, 2014.
[4] M. Giger, N. Karssemeijer, J. Schnabel, Breast image analysis for risk assessment, detection, diagnosis, and treatment of cancer, Annu. Rev. Biomed. Eng. 15 (2013) 327–357.
[5] A. Gastounioti, E.F. Conant, D. Kontos, Beyond breast density: a review on the advancing role of parenchymal texture analysis, Breast Cancer Res. 18 (91) (2016).
[6] J.O.P. Wanders, C.Hv. Gils, N. Karssemeijer, K. Holland, M. Kallenberg, P.H.M. Peeters, M. Nielsen, M. Lillholm, The combined effect of mammographic texture and density of breast cancer risk: a cohort study, Breast Cancer Res. 20 (36) (2018).
[7] D. Kontos, S.J. Winham, A. Oustimov, L. Pantalone, M.-K. Hsieh, A. Gastounioti, D.H. Whaley, C. Hruska, K. Kerlikowske, K. Brandt, E. Conant, C.M. Vachon, Radiomic phenotypes of mammographic parenhcymal complexity: toward augmenting breast density in breast Cancer risk assessment, Radiology 290 (1) (2018) 41–49.
[8] S. Pertuz, G.F. Torres, R. Tamimiy, J. Kamarainen, Open framework for mammography-based breast cancer risk assessment, D IEEE EMBS International Conference in Biomedical and Health Informatics, Chicago (2019).
[9] A. Yala, C. Lehman, T. Schuster, T. Portnoi, R. Barzilay, A deep learning mammography-based model for improved breast Cancer risk prediction, Radiology 292 (1) (2019).
[10] M. Kallenberg, K. Petersen, M. Nielsen, A.Y. Ng, P. Diao, C. Igel, C. Vachon, K. Holland, R.R. Winkel, N. Karssemeijer, M. Lillholm, Unsupervised deep learning applied to breast density segmentation and mammographic risk scoring, IEEE Trans. Med. Imaging 35 (5) (2016) 1322–1331.
[11] S. Rivetti, N. Lanconelli, R. Campanini, M. Bertolini, G. Borasi, A. Nitrosi, C. Danielli, L. Angelini, S. Maggi, Comparison of different commercial FFDM units by means of physical characterization and contrast-detail analysis, Med. Phys. 33 (11) (2006) 4198–4209.
[12] J. Wei, H.-P. Chan, Y.-T. Wu, C. Zhou, M.A. Helvie, A. Tsodikov, L.M. Hadjiiski, B. Shainer, Association of computerized mammographic parenhcymal pattern measure with breast cancer risk: a pilot case-control study, Radiology 260 (1) (2011) 42–49.
[13] Y. Zheng, B.M. Keller, S. Ray, Y. Wang, E.F. Conant, J.C. Gee, D. Kontos, Parenchymal texture analysis in digital mammography: a fully automated pipeline for breast cancer risk assessment, Med. Phys. 42 (7) (2015) 4149–4160.
[14] H. Li, M. Giger, L. Lan, J. Janardanan, C.A. Sennet, Comparative analysis of image-based phenotypes of mammographic density and parenchymal patterns in distinguishing between BRCA1/2 cases, unilateral cancer cases, and controls, J. Med. Imaging 1 (3) (2014).
[15] L. Haberle, F. Wagner, P. Fasching, S.M. Jud, K. Heusinger, C.R. Loehberg, Characterizing mammographic images using generic texture features, Breast Cancer Res. 14 (2) (2012) R59.
[16] O. Araque, M.P. Mejia-Sandoval, A. Sassi, K. Holli-Hellenius, A.-L. Laaperi, I. Rinta-Kiikka, O. Arponen, S. Pertuz, Selecting the mammographic-view for the parenchymal analysis-based breast cancer risk assessment, De IEEE-EMBS International Conference on Biomedical and Health Informatics, Chicago (2019).
[17] M. Nielsen, C.M. Vachon, C.G. Scott, K. Chernoff, G. Karemore, N. Karssemeijer, M. Lillholm, M.A. Karsdal, Mammographic texture resemblance generalizes as an independent risk factor for breast cancer, Breast Cancer Res. 16 (R37) (2014).
[18] A. Manduca, M.J. Carston, J.J. Heine, C.G. Scott, V.S. Pankratz, K.R. Brandt, T.A. Sellers, C.M. Vachon, J.R. Cerhan, Texture features from mammographic images and risk of breast cancer, Cancer Epidemiol. Biomarkers Prev. 18 (3) (2009) 837–845.
[19] B. Keller, D. Nathan, Y. Wang, Y. Zheng, J.C. Gee, E. Conant, D. Kontos, Estimation of breast percent density in raw and processed full field digital mammography images via adaptive fuzzy c-means clustering and support vector machine segmentation, Med. Phys. 39 (8) (2012) 4903–4917.
[20] J.W. Byng, N.F. Boyd, E. Fishell, R.A. Jong, M.J. Yaffe, The quantitative analysis of mamographic densities, Phys. Med. Biol. 39 (10) (1994) 1629–1638.
[21] N.F. Boyd, L.J. Martin, M. Bronskill, M.J. Yaffe, N. Duric, S. Minkin, Breast tissue composition and susceptibility to breast cancer, J. Natl. Cancer Inst. 102 (16) (2010) 1224–1237.
[22] K. Kerlikowske, W. Zhu, A.N.A. Tosteson, B.L. Sprague, J.A. Tice, C.D. Lehman, D.L. Miglioretti, Identifying women with dense breasts at high risk of interval cancers, Ann. Intern. Med. 162 (10) (2015) 673–681.
[23] G.E.P. Box, D.R. Cox, An analysis of transformations, Royal Statistical Society Series B (26) (1964) 211–252.
[24] J.L. Hopper, Odds per adjusted standard deviation: comparing strenghts of associations for risk factors measured on different scales and across diseases and populations, Am. J. Epidemiol. 182 (10) (2015) 863–867.
[25] T.L. Nguyen, Y.-H. Choi, Y.K. Aung, C.F. Evans, N.H. Trinh, S. Li, G.S. Lite, M.-S. Kim, P.C. Brennan, M.A. Jenkins, J. Sung, Y.-M. Song y, J.L. Hopper, Breast cancer risk associtions with digital mammographic density by pixel brightness threshold and mammographic system, Radiology 286 (2) (2018) 433–442.
[26] E.R. DeLong, D.M. DeLong, D.L. Clarke-Pearson, Comparing the areas under two or more correlated receiver operating characteristic curves: a nonparametric approach, Biometrics 44 (1988) 837–845.
[27] E.B. Claus, J.M. Schidkraut, W.D. Thompson, N.J. Risch, The genetic attributable risk of breast and ovarian cancer, *Cancer* 77 (11) (1996) 2318–2324.
[28] V.A. McCormack, Id.S. Silva, Breast density and parenchymal patterns as markers of breast cancer risk: a metaanalysis, Cancer Epidemiol. Biomark. Prev. 1169 (2006) 1159.
[29] Volpara Solutions, https://volparasolutions.com/our-products/volparadensity/, [En línea]. Available: https://volparasolutions.com/our-products/volparadensity/. [Último acceso: 31 01 2019].
[30] B.M. Keller, J.C.D. Daye, E.F. Conant, D. Kontos, Preliminary evaluation of the publicly available Laboratory for Breast Radiodensity Assessment (LIBRA) software tool: comparison of fully automated area and volumetric density measures in a case-control study with digital mammography, Breast Cancer Res. 17 (117) (2015).
[31] Hologic, Quantra 2.2 Breast Density Assessment Software, (2018) [En línea]. Available: https://www.3dimensionssystem.com/density-assessmen t. [Último acceso: 20 12 2018].
[32] S. Pati, S. Bakas, A. Sotiras, R. Kalarot, P. Sridharan, M. Bergman, S. Rathore, H. Akbari, P. Kushkevich, T. Shinohara, Y. Fan, D. Kontos, R. Verman, C. Davatzikos, Cancer imaging phenotypes toolkit (CaPTk): a radio(geno)mics software platform leveraging quantitative image analystics for computational oncology, De 103rd Scientific Assembly and Annual Meeting of the Radiological Society of North America (RSNA), Chicago (2017).
[33] S. Pati, S. Rathore, R. Kalarot, P. Sridharan, M. Bergman, T. Shinohara, P. Yushkevich, Y. Fan, R. Verma, D. Kontos, C. Davatzikos, Cancer and phenomics toolkit (CaPTk): a software suite for computational oncology and radiomics, De 102nd Scientific Assembly and Annual Meeting of the Radiological Society of North America (RSNA), Chicago (2016).
[34] C. Davatzikos, S. Rathore, S. Bakas, S. Pati, M. Bergman, R. Karalot, P. Sridharan, A. Gastounioti, N. Jahani, E. Cohen, H. Akbrai, B. Tunc, J. Doshi, D. Parker, M. Hsieh, A. Sotiras, H. Li, Y. Ou, R.K. Doot, M. Bilello, Y. Fan, R. Shinohara, D. Kontos, Cancer imaging phenomics toolkit: quantitative imaging analytics for precision diagnostics and predictive modeling of clinical outcome, J. Med. Imaging

5 (1) (2018).
[35] A. Gastounioti, A. Oustimov, B.M. Keller, L. Pantalone, M.K. Hsieh, E.F. Conant, D. Kontos, Breast parenchymal patterns in processed versus raw digital mammograms: A large population study toward assessing differences in quantitative measures across image representations, Med. Phys. 43 (11) (2016) 5862–5877.
[36] K.-H. Ng, C.-H. Yip, N.A.M. Taib, Standaridisation of clinical breast-density measurement, Lancet 13 (4) (2012) 334–336.
[37] E.A. Ooms, H.M. Zonderland, M.J.C. Eikemans, M. Kriege, B.M. Delavary, C.W. Burger, A.C. Ansink, Mammography: interobserver variability in breast density assessment, Breast 16 (6) (2007) 568–576.
[38] American Cancer Society, Cancer Facts and Figures 2015, American Cancer Society, 2015 [En línea]. Available: https://www.cancer.org/content/dam/cancer-org/research/cancer-facts-and-statistics/annual-cancer-facts-and-figures/2015/cancer-facts-and-figures-2015.pdf . [Último acceso: 2018 12 17].
[39] N. Howlader, A.M. Noone, M. Krapcho, D. Miller, K. Bishop, C.L. Kosary, M. Yu, J. Ruhl, Z. Tatalovich, A. Mariotto, D.R. Lewis, H.S. Chen, E.J. Feuer, K.A. Cronin, SEER Cancer Statistics Review, 1975-2014, (2017) [En línea]. Available: https://seer.cancer.gov/archive/csr/1975_2014/ . [Último acceso: 30 11 2018].